ИНСТИТУТ ЯДЕРНОЙ ФИЗИКИ СО АН СССР

S.I.Dolinsky, V.P.Druzhinin, M.S.Dubrovin,
S.I.Eidelman, V.B.Golubev, V.N.Ivanchenko,
P.M.Ivanov, G.YA.Kezerashvili, I.A.Koop,
A.P.Lysenko, E.V.Pakhtusova, E.A.Perevedentsev,
A.N.Peryshkin, A.A.Polunin, I.YU.Redko,
S.I.Serednyakov, YU.M.Shatunov, V.A.Sidorov,
A.N.Skrinsky, YU.V.Usov, I.B.Vasserman,
P.V.Vorobyov

RESULTS OF THE EXPERIMENTS FROM THE NEUTRAL DETECTOR AT THE VEPP-2M STORAGE RING IN THE ENERGY REGION $2E_0 = 1.05 - 1.40$ GeV

PREPRINT 85-98

НОВОСИБИРСК

ABSTRACT

Results of the experiments with the Neutral Detector at e^+e^- storage ring VEPP-2M at c.m. energy 1.05—1.40 GeV are presented. The results are based on integrated luminosity of 3 pb^{-1}. The cross sections of the reactions $e^+e^-\to\omega\pi^0$, $\pi^+\pi^-\pi^0$, $\eta\pi^+\pi^-$ are measured and found to be significantly higher than simple Vector Dominance Model predictions with only ϱ-, ω- and Φ-mesons taken into account. The QED processes $e^+e^-\to e^+e^-e^+e^-$, $e^+e^-\gamma\gamma$ and $\gamma\gamma\gamma$ were observed where all the angles between final particles are large.

The experiments were performed using the Neutral Detector at e^+e^- storage ring VEPP-2M [1]. Data were collected in the center-of-mass energy range 1.05—1.40 GeV with an integrated luminosity of 3 pb^{-1}. The Neutral Detector is a calorimeter with NaI(Tl) crystals. It has been described in detail elsewhere [2]. The data taking and preliminary results have been presented in [3]. Here we present the results of further analysis of experimental data.

1. INVESTIGATION OF THE PROCESS $e^+e^-\to\omega\pi^0$

The reaction $e^+e^-\to\pi^+\pi^-\pi^0\pi^0$ was studied earlier in the energy range below 1.4 GeV [4, 5]. It was shown, that this reaction proceeds through the $\omega\pi^0$, $A_1\pi$ and $\varrho\pi\pi$ intermediate states wich are difficult to separate. Here we analyse the data on the process

$$e^+e^-\to\omega\pi^0\to\pi^0\pi^0\gamma \qquad (1.1)$$

using greater statistics compared to [3].

The following criteria were applied to select the events of the process (1.1):

—four or five photons are detected;
—total energy deposition is greater than $1.3E_0$, where E_0 is a beam energy;
—total transverse momentum of all photons is less than 150 MeV;
—the most energetic photon does not deposit in any NaI(Tl) layer more than 75% of its energy;
—angle between any two photons is greater than 15°.

These criteria completely remove the background caused by cosmic rays, particles lost from the beams and significantly suppress the background from neutral decays of Φ-meson. Further analysis has been done separately for 343 four-photon and 182 five-photon events thus selected.

For five-photon events the kinematical fit [2] was checked with additional requirement, that there must be two π^0 mesons in each event. The corresponding $\pi^0\gamma$-mass spectrum for 117 events thus selected is shown in Fig.1,*a* (two entries per event). In 99 events one of the masses is close to ω-meson mass. The energy dependence of the corresponding visible cross section is shown in Fig.2,*a* and Table 1.

Table 1

Cross Sections of the Reaction $e^+e^-\to\omega\pi^0$

E_0, MeV	$\sigma_{vis}^{4\gamma}$, pb	$\sigma_{vis}^{5\gamma}$, pb	σ_{QED}, pb	σ_Φ, pb	$\sigma_{tot}^{\omega\pi^0}$, nb
1020	—	—	—	—	9.1±1.3
1050	92	15	9	14	8.5±3.2
1070	36	60	8	7	8.3±2.9
1090	89	15	8	5	9.2±3.5
1110	180	49	8	4	22.0±5.9
1130	92	26	8	3	11.0±3.7
1150	100	38	7	2	13.0±3.9
1170	57	43	7	2	9.4±3.5
1190	49	12	7	2	7.8±2.9
1210	113	51	7	1	11.1±2.4
1230	51	72	6	1	13.8±3.7
1250	66	92	6	1	15.3±4.4
1270	92	35	6	1	16.7±4.3
1290	88	46	6	1	9.4±1.9
1310	91	50	6	1	13.4±2.4
1330	74	25	6	0	13.8±2.9
1350	75	47	5	0	8.9±2.0
1370	98	54	5	0	13.2±2.3
1390	91	25	5	0	14.7±2.2

For four-photon events no kinematical fit required. For further analysis the events with at least one π^0-meson were selected. The spectra of the mass recoiling against π^0-meson and $\pi^0\gamma$ mass for these 280 events are shown in Fig.1. The peak at the ω-meson mass is clearly seen. This allows to select 199 events of the reaction (1.1). The energy dependence of the corresponding visible cross section is presented in Fig.2,*b* and Table 1. The background arises primarily from the neutral decays of Φ-meson and QED process [6]:

$$e^+e^-\to\gamma\gamma\gamma\gamma \qquad (1.2)$$

Since the cross sections obtained for four- and five-photon events are in agreement, we further consider their sum and parametrize its energy dependence by the formula:

$$\sigma_{viz}(E)=\varepsilon\cdot B(\omega\to\pi^0\gamma)\cdot\sigma(E)+\sigma_\Phi(E)+\sigma_{QED}(E), \qquad (1.3)$$

where $\sigma(E)$ is a total cross section for the process (1.1), $\sigma_{QED}(E)$ is the calculated visible cross section for the process (1.2) (cf. Table 1), ε is a detection efficiency equal to $(11.4\pm1.2)\%$ independently of the energy, $\sigma_\Phi(E)$ is the Breit-Wigner cross section for neutral Φ-meson decays (Table 1) with parameters obtained from the analysis of four- and five-photon events recorded in previons Φ-meson experiment [7] using the selection criteria described above.

Taking $B(\omega\to\pi^0\gamma)=(8.7\pm0.5)\%$ [8], one can obtain from (1.3) the total cross section of the process (1.1) shown in Fig.2,*c* and Table 1. The energy dependence of the cross section was approximated using standard Vector Dominance Model with ϱ(770) only [9]:

$$\sigma(E)=12\pi\left(\frac{m_\varrho}{2E}\right)^3\frac{\Gamma(\varrho\to e^+e^-)\Gamma(\varrho\to\omega\pi^0)}{(4E^2-m_\varrho^2)^2+(m_\varrho\Gamma_\varrho(E))^2},$$

$$\Gamma(\varrho\to\omega\pi^0)=\frac{g_{\omega\varrho\pi}^2}{4\pi}\frac{p_\omega^3}{3},$$

$$p_\omega=\sqrt{\frac{(4E^2-m_\omega^2-m_\pi^2)^2-4m_\omega^2m_\pi^2}{16E^2}}, \qquad (1.4)$$

$$\Gamma_\varrho(E)=\Gamma_\varrho(m_\varrho)\cdot\left(\frac{4E^2-4m_\pi^2}{m_\varrho^2-4m_\pi^2}\right)^{3/2}\cdot\frac{m_\varrho}{2E}.$$

The only free parameter here was the coupling constant $g_{\omega\varrho\pi}^2/4\pi$. The following value for it has been obtained:

$$g_{\omega\varrho\pi}^2/4\pi=28\pm4\ \text{GeV}^{-2}. \qquad (1.5)$$

The error here is due to systematic error of the Monte-Carlo simulation (10%) and uncertainty of the $B(\omega\to\pi^0\gamma)$. This value of the coupling constant is noticeably higher than $g^2_{\omega\varrho\pi}/4\pi=20$ GeV^{-2} predicted by VDM [9]. Recent QCD calculations [10] also yield the smaller value $g^2_{\omega\varrho\pi}/4\pi=23$ GeV^{-2}. The discrepancy observed can be due to the contributions of the higher-lying resonances. We are planning to perform data analysis taking them into account, as well as continue a study of the reaction $e^+e^-\to\omega\pi^0$ using the main mode of the ω-meson decay.

2. REACTION $e^+e^-\to\pi^+\pi^-\pi^0$

The reaction

$$e^+e^-\to\pi^+\pi^-\pi^0 \qquad (2.1)$$

was studied earlier at the energies lower than 1.1 GeV at ACO storage ring [11] and higher than 1.35 GeV at DCI [12] (Fig.5). No measurements have been done yet in the energy range 1.1—1.35 GeV. In the Vector Dominance Model [13] the reaction (2.1) is described by the diagram of Fig.3, in which the ω, $\Phi\to\varrho\pi$ transition is dominant. The calculated cross section of the process with the energy dependence of widths of resonances taken into account is equal to 7 nb at c.m. energy 1.05 GeV and decreases to 0.3 nb at 1.4 GeV.

Events of the process (2.1) were selected by applying the following criteria:

—there must be two charged particles and two photons detected in shower chambers in the event;
—energy and momentum must be balanced within the experimental accuracy;
—the invariant mass of two photons $M_{\gamma\gamma}$ must be compatible with π^0-mass ($110<M_{\gamma\gamma}<160$ MeV).

The invariant mass distribution for the events thus selected (Fig.4,*a*) shows a prominent peak at π^0-mass in agreement with the Monte-Carlo simulation (Fig.4,*b*). The main background is due to reaction $e^+e^-\to\pi^+\pi^-\pi^0\pi^0$ (Fig.4,*c*). Its subtraction was done by using the number of events in the effective mass ranges 85—110 and 160—185 MeV. The total number of events after background subtraction was about 550. The detection efficiency for the reaction (2.1) with the selection criteria described above is about 5%. In

Fig.5 the energy dependence of the measured cross section as well as calculated one is shown. Our results are in agreement with the previous experiments, but are based on higher statistics. The average cross section in this energy range is equal to 3.6±0.4 nb, that is much higher than VDM prediction. This discrepancy is possibly caused by multihadron intermediate states [14], electromagnetic ϱ—ω mixing [13] or by contribution of higher-lying resonances, for example $\Phi'(1680)$.

3. QED PROCESSES OF THE FOURTH ORDER IN α

The validity of QED was tested in two different types of experiments:

—precise measurements of lepton magnetic moments, Lamb shift etc., where high orders in α at small momentum transfers were tested;
—experiments at high energy with colliding beams studying processes of the second order in α e.g. $e^+e^-\to e^+e^-$, $e^+e^-\to\mu^+\mu^-$ where QED at high momentum transfer is tested.

In this paper the processes of the fourth order in α at relatively large momentum transfers are studied:

$$e^+e^-\to e^+e^-e^+e^- , \qquad (3.1)$$

$$e^+e^-\to e^+e^-\gamma\gamma , \qquad (3.2)$$

$$e^+e^-\to\gamma\gamma\gamma\gamma . \qquad (3.3)$$

The investigation of these reactions in colliding beams experiments is of interest for several reasons. It allows to check QED for higher order in α comparing QED predictions with measured differential cross sections. In the final states of these reactions new hypothetical particles like charged or neutral leptons may manifest themselves [16, 17], affecting the invariant mass spectra of final particles. Furthermore, the reactions under study may cause a background for rare hadronic processes. The reaction (3.1) was earlier observed at PEP and PETRA with total statistics of 10 events [18—22]. The reactions (3.2) and (3.3) were not observed up to now. At present time the calculations have been done for all processes (3.1—3.3) [6, 23—26], however it is still difficult to compare them with the experimental data because of computational difficulties.

To look for the processes (3.1—3.3) we imposed following selection criteria:

—an angle between each particle and the beam axis exceedes 45°;
—the energy and momentum are balanced within the experimental accuracy;
—spatial angle between any two particles exceedes 20°;
—each particle has an energy higher than $0.04E_0$;
—the procedure of e/π separation [15] is used to suppress the π-meson background;
for the reaction (3.2) an additional cut is imposed. Each photon must have an energy higher than $0.14E_0$ and fire a shower chamber.

These criteria reduced the sample to 11 events of the reaction (3.1) and 45 events of the reaction (3.2). The energy dependence of the cross sections for these reactions is consistent with expected E^{-2} (Fig.6). The estimated background due to hadronic reactions $e^+e^-\to\pi^+\pi^-\pi^+\pi^-$, $e^+e^-\to\pi^+\pi^-\pi^0\pi^0$ etc. is less than 10% of a visible cross section.

To obtaine the differential cross section of the processes (3.1) and (3.2) integrated over the detector acceptance, we are planning to carry out Monte-Carlo simulation based on the results of Refs [25, 26].

To search for the process (3.3), 283 four-photon events were selected in which at least three photons fired shower chambers. The most of them were due to the reaction (1.1). Its contribution was reduced using the difference between (1.1) and (3.3) in two- or three-photon invariant mass spectra. For this purpose the events with π^0-mesons were isolated by the requirement, that at least one photon pair had an invariant mass $M_{\gamma\gamma}=135\pm70$ MeV, and processed separately. In such events invariant masses of all $\pi^0\gamma$ sets as well as π^0-mesons recoil masses were calculated. All the events, in which at least one mass calculated was in the interval 660—900 MeV, close to ω-meson mass, were removed. This cut reduced several times the contribution of the reaction (1.1). The remaining background was subtracted using Monte-Carlo simulation. The detection efficiency for the reaction (3.3) and some other data are listed in the Table 2. The measured total cross section (Fig.7) of the process (3.3) is in agreement with QED expectations [6].

Table 2

Detection Efficiency and Cross Section of the Reaction $e^+e^-\to\gamma\gamma\gamma\gamma$ (QED)

E_0, MeV	L, pb^{-1}	$\sigma_{tot}^{\omega\pi^0}$ nb	$\varepsilon^{\omega\pi^0}\cdot B_{\omega\to\pi\gamma}$, %	$\varepsilon_{QED}^{4\gamma}$, %	N_{ex}	$N^{\omega\pi^0}$	$N_{QED}^{4\gamma}$	$\sigma_{QED}^{4\gamma}$, pb
1100	0.378	12.0±2	0.14	2.33	4	6	0+3	0+340
1200	0.581	10.4±2	0.14	6.77	15	8.4	7±5	178±130
1300	1.442	13.7±2	0.14	6.50	42	27	15±8	154±80
1400	0.860	12.3±2	0.14	6.38	17	15	2^{+5}_{-2}	36^{+90}_{-36}

In this paper we present the first observation of the processes (3.2) and (3.3) when all the particles are produced at large angles. In future we intend to increase statistics considerably and to compare invariant mass spectra of the final particles with QED predictions.

4. REACTION $e^+e^-\to\eta\pi^+\pi^-$

The reaction

$$e^+e^-\to\eta\pi^+\pi^- \qquad (4.1)$$

is determined by isovector part of electromagnetic current $e^+e^-\to\varrho,\varrho',\ldots\to\eta\pi^+\pi^-$. Vector Dominance Model [27] predicts a rapid growth of the cross section at a total energy above the threshold of the reaction $e^+e^-\to\varrho\to\eta\varrho\to\eta\pi^+\pi^-$. The cross section increases by a factor of 25 in the c.m. energy range 1.2—1.4 GeV and reaches the value of the 0.25 nb. Furthermore, in the reaction (4.1) one can expect manifestations of the $\varrho(1250)$ meson, the existence of which is discussed for many years. At last, recently a narrow peak in $\eta\pi^+\pi^-$ system with the mass of 1.28±0.01 GeV and width of 0.08±0.01 GeV was observed in photoproduction experiment [28]. The analysis carried out in Ref. [28] indicated that quantum numbers of this state may be the same as photon ones, hence it may be produced in e^+e^- collisions.

The search for the process (4.1) was performed for the decay mode $\eta\to\gamma\gamma$. Events with two charged particles and two photons with an invariant mass $M_{\gamma\gamma}$ greater than 300 MeV were selected.

Then, using the kinematical fit [2], we removed events with insufficient energy-momentum balance.

The main background for the reaction (4.1) is caused by

$$e^+e^- \to \omega\pi^0,\ A_1\pi,\ \varrho\pi\pi \to \pi^+\pi^-\pi^0\pi^0\ . \qquad (4.2)$$

Its cross section is about 40 nb in the energy range 1.1—1.4 GeV, which is by more than two orders of magnitude greater than the cross section of (4.1). Using Monte-Carlo simulation the detection efficiency for the reaction (4.1) was determined to be $(9\pm2)\%$. The expected two-photon invariant mass srectra for the reactions (4.1) and (4.2) are shown in Fig.8. The same distributions for selected events are shown in Fig.9 separately for c.m. energy regions 1.05—1.3 GeV and 1.3—1.4 GeV. There is no statistically significant peak at η-meson mass in Fig.9,*a*, while an enhancement of 1.5 standard deviations is seen in Fig.9,*b*.

For background subtraction we separated three regions in $M_{\gamma\gamma}$ (Fig.9). The interval $530<M_{\gamma\gamma}<570$ MeV contains the most the of process (4.1), while the intervals $490<M_{\gamma\gamma}<530$ MeV and $570<M_{\gamma\gamma}<610$ MeV contain mostly the process (4.2) and were used to calculate background which was further statistically subtracted. Then, taking into account the detection efficiency, cross section of (4.1) was obtained (Fig.10). One can see, that only in the energy interval 1.36—1.40 GeV, cross section significantly differs from zero and exceeds VDM prediction [27] based on $\varrho(770)$ contribution only. Our result is in agreement with DM1 data [29] at higher energy 1.4—2.8 GeV (Fig.10), indicated that main contribution to the reaction (4.1) in this region is caused by $\varrho'(1600)$.

The resonance with the mass of 1.28 GeV and width of 0.08 GeV [28] is not seen, so we can obtain only upper limit on the product of its electron width and branching ratio into $\eta\pi^+\pi^-$:

$$\Gamma_{e^+e^-}\cdot B_{\eta\pi^+\pi^-}<6\ \text{eV}\ (90\%\ \text{C.L.})$$

REFERENCES

1. *Tumaikin G.M.* Proceedings of the 10-th International Conference on High Energy Particle Accelerators. Serpukhov, 1977, vol.1, p.443.
2. *Golubev V.B. et al.* Nucl. Instr. and Methods 227 (1984) 467.
3. *Druzhinin V.P. et al.* Preprint INP 84-93. Novosibirsk, 1984.
4. *Kurdadze L.M. et al.* Preprint INP 79-69. Novosibirsk, 1979.
5. *Cosme G. et al.* Phys. Lett. 63B (1976) 349.
6. *Berends F.A. et al.* Nucl. Phys. B239 (1984) 395.
7. *Druzhinin F.A. et al.* Preprint INP (to be published).

8. Review of Particle Properties. Particle Data Group, 1984.
9. *Karnakov V.E.* Submitted to Yadernaya Fizika.
10. *Eletskiy V.L., Kogan Ya.I.* Yadernaya Fizika 39 (1984) 138.
11. *Cordier A. et al.* Nucl. Phys. B172 (1980) 13.
12. *Augustin J.E. et al.* Preprint LAL/83-21. Orsay, 1983.
    Paulot C. Preprint LAL/79-14. Orsay, 1979.
13. *Achasov N.N. et al.* Phys. Lett. 50B (1974) 448.
14. *Baier V.N., Fadin V.S.* Pisma v ZhETP 15 (1972) 219.
15. *Golubev V.B. et al.* Report at the 3-rd International Conference on Colliding Beam Instrumentation. Novosibirsk, 1984.
16. *Gornau M. et al.* Phys. Rev. D29 (1984) 2539.
17. *Thun R.* Phys. Lett. 134B (1984) 459.
18. *Perl M.L. et al.* Preprint SLAC-PUB-3515. Massachusetts, 1984.
19. *Adeva B. et al.* Phys. Rev. Lett. 48 (1982) 721.
20. *Ford W.T. et al.* Preprint SLAC-PUB-3016. Wisconsin, 1982.
21. *Bartel W. et al.* Z. Phys. C24 (1984) 223.
22. *Behrend H.J. et al.* Preprint DEZY 84-103. Hamburg, 1984.
23. *Berends F.A. et al.* Preprint KUL-TF-84/7.
24. *Kuraev E.A. et al.* Preprint INP 85-69. Novosibirsk,1985.
25. *Kleiss R.* Nucl. Phys. B241 (1984) 61.
26. *Kuraev E.A. et al.* Submitted to Yadernaya Fizika.
27. *Achasov N.N., Karnakov V.A.* Pisma v ZhETP 39 (1984) 285.
28. *Atkinson M., Axon T.J. et al.* Nucl. Phys. B242 (1984) 269.
29. *Delcourt B., Bisello D. et al.* Phys. Lett. 113B (1982) 93.

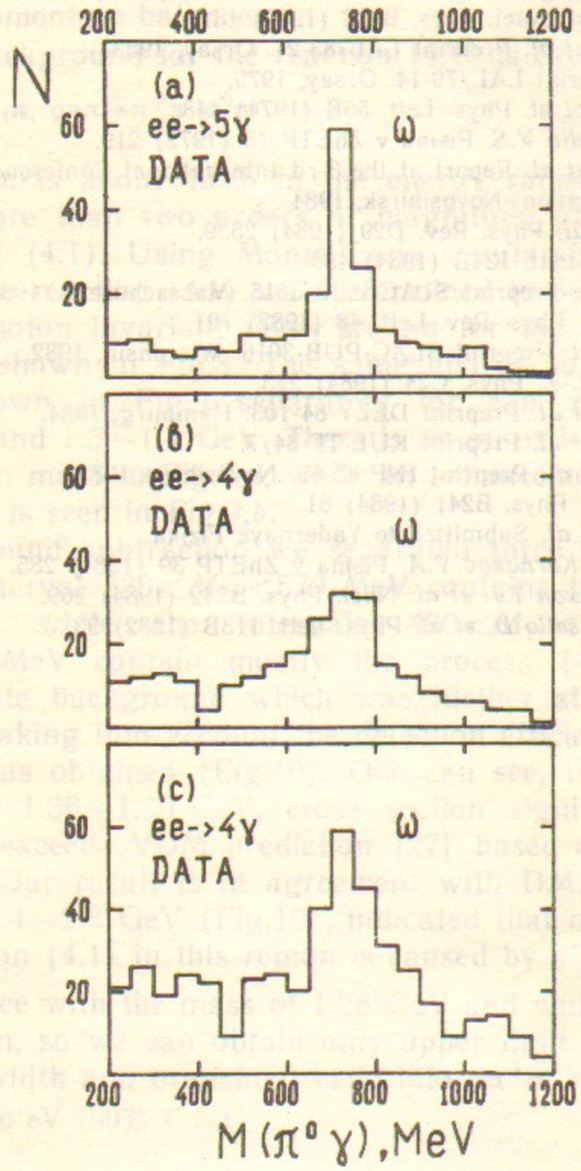

Fig.1. Selection of the events with ω-meson using invariant mass spectra:
a—spectrum of $\pi^0\gamma$-invariant masses in five-photon events; *b*—spectrum of π^0-meson recoil masses in four-photon events; *c*—$\pi^0\gamma$-invariant mass spectrum for four-photon events.

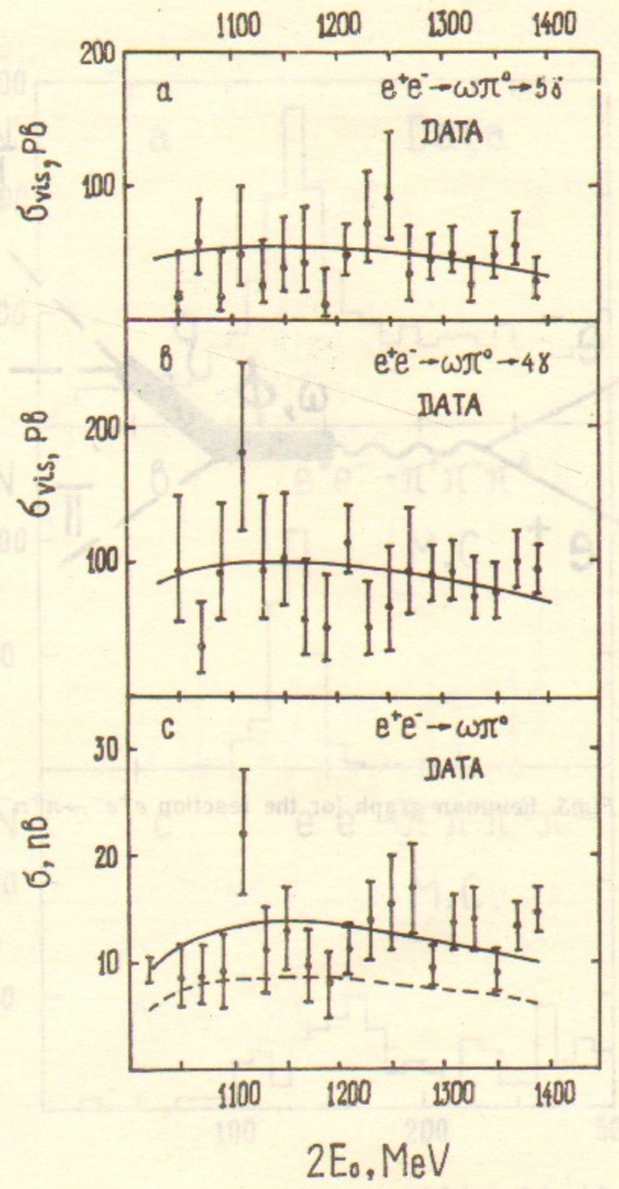

Fig.2. Cross section for selected $\omega\pi^0$ events:
a—visible cross section for five-photon events; *b*—visible cross section for four-photon events; *c*—total cross section of $e^+e^-\to\omega\pi^0$. Solid line—the optimal curve, dotted line is the calculated ρ(770) contribution [9].

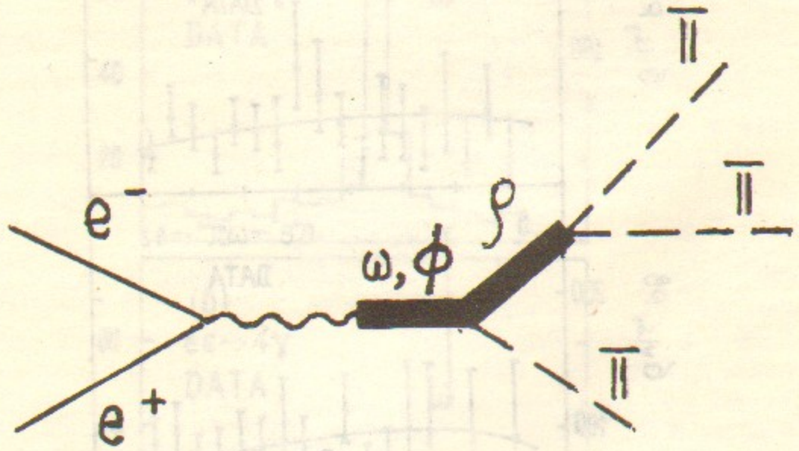

Fig.3. Feinman graph for the reaction $e^+e^-\to\pi^+\pi^-\pi^0$.

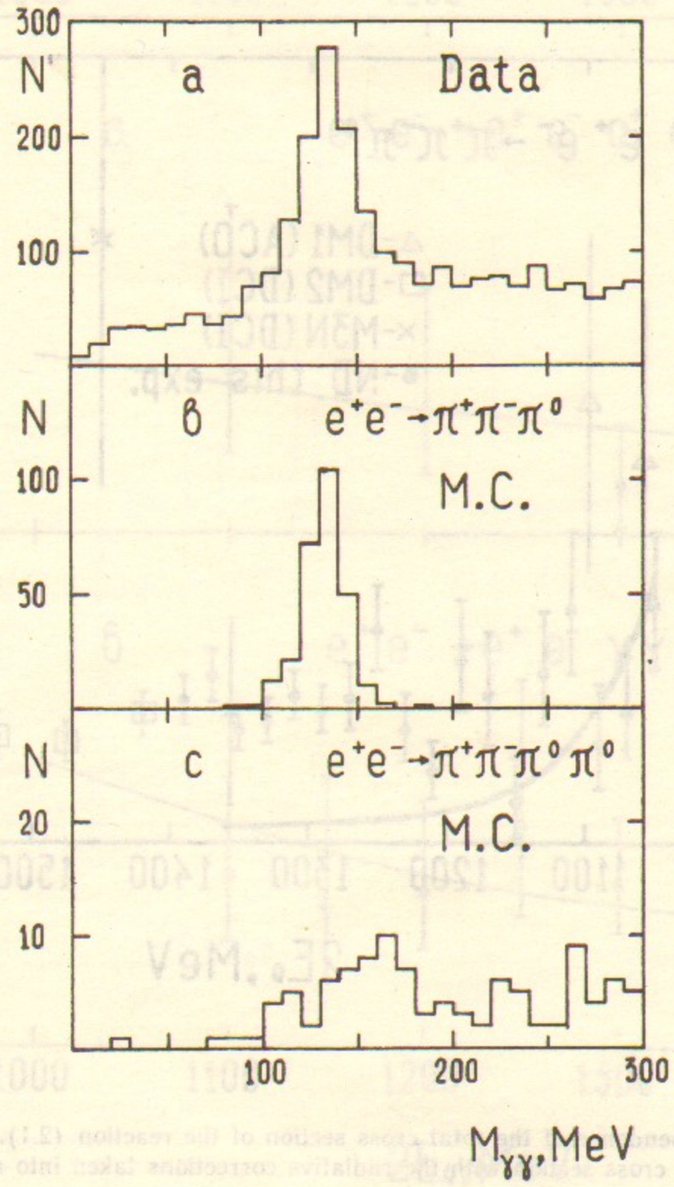

Fig.4. Two-photon invariant mass distributions for the process (2.1):
a—experimental data; *b*— simulation of the reaction (2.1); *c*—simulation of the reaction $e^+e^-\to\pi^+\pi^-\pi^0\pi^0$.

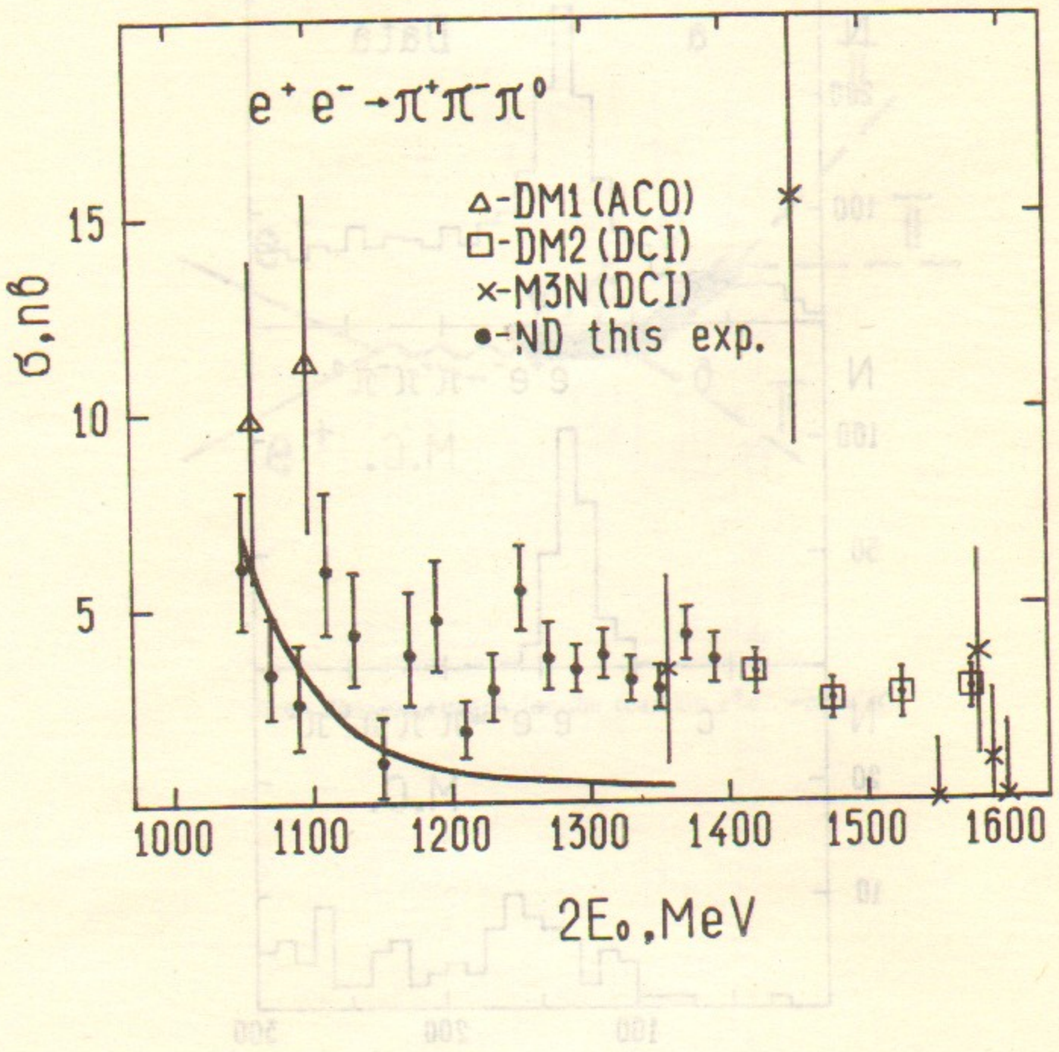

Fig.5. Energy dependence of the total cross section of the reaction (2.1). Solid line is a calculated cross section with the radiative corrections taken into account.

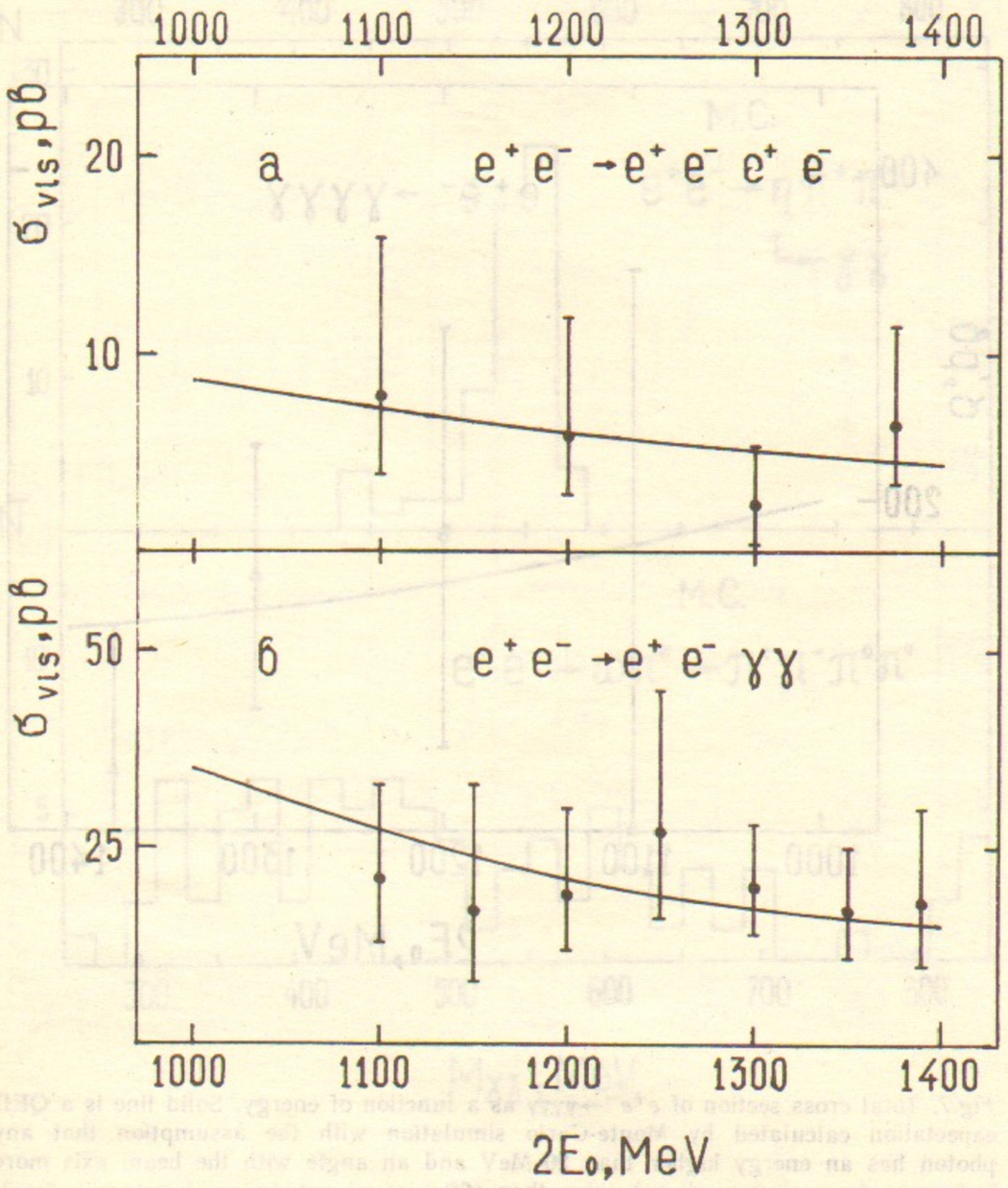

Fig.6. Energy dependence of the visible cross sections $e^+e^- \to e^+e^-e^+e^-$ (*a*) and $e^+e^- \to e^+e^-\gamma\gamma$ (*b*).

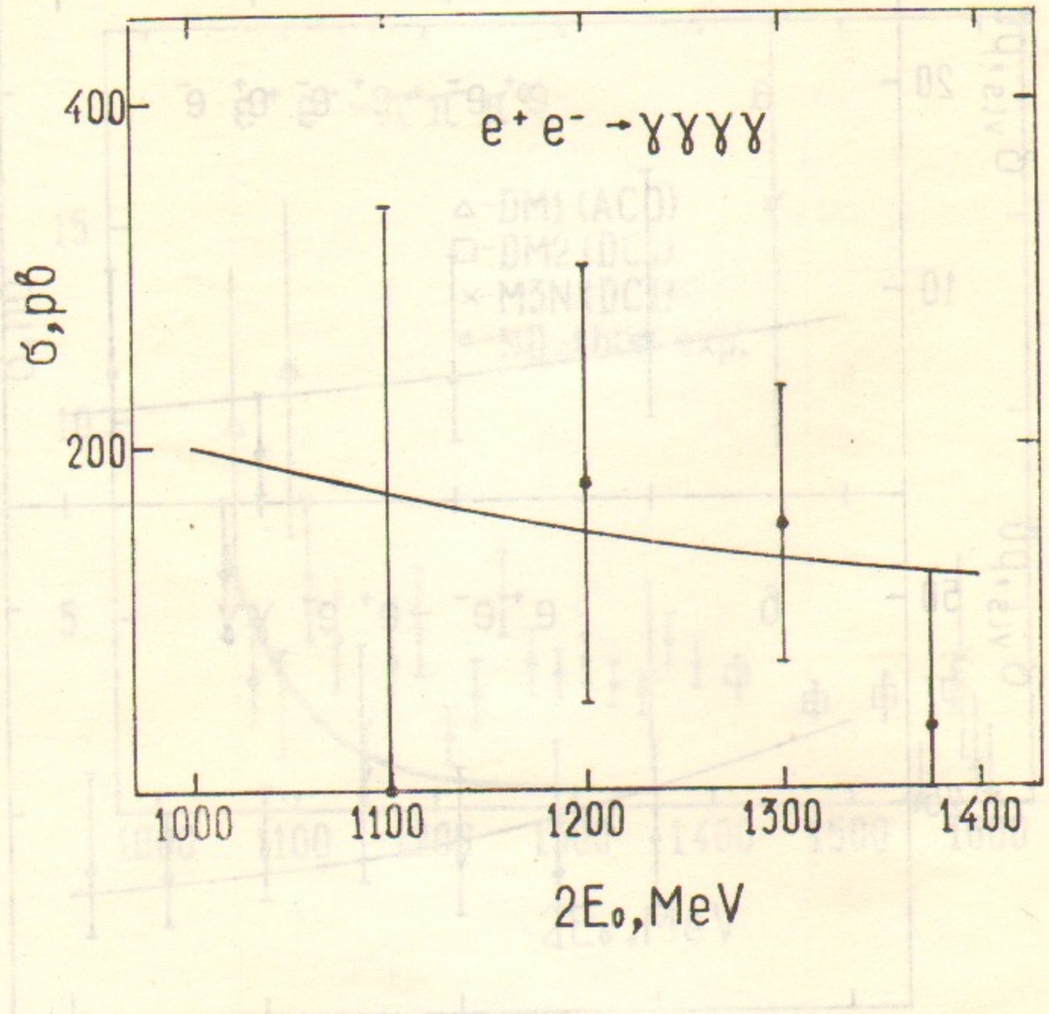

Fig.7. Total cross section of $e^+e^- \to \gamma\gamma\gamma\gamma$ as a function of energy. Solid line is a QED expectation calculated by Monte-Carlo simulation with the assumption that any photon has an energy higher than 20 MeV and an angle with the beam axis more than 40°.

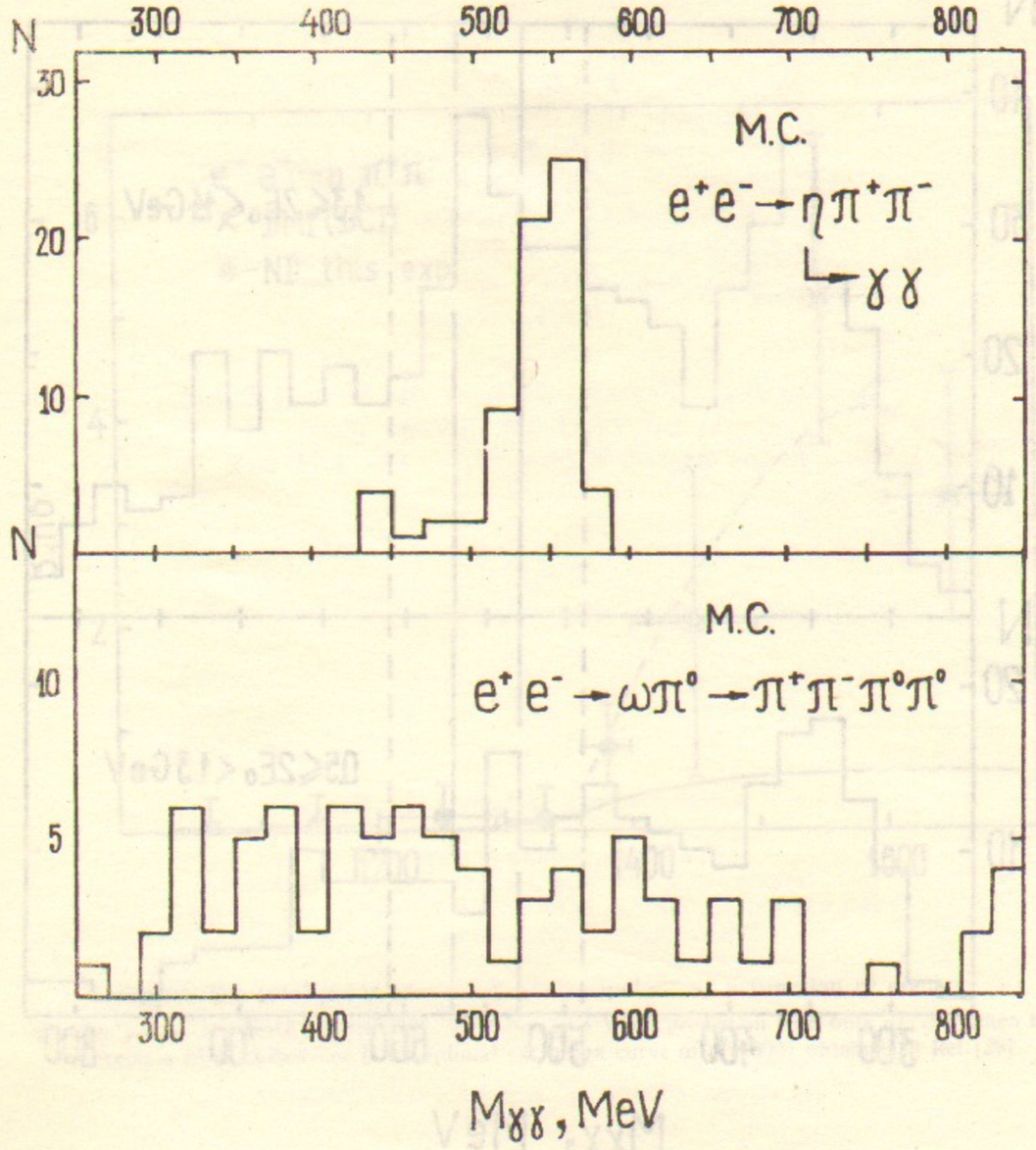

Fig.8. Simulated two-photon invariant mass spectra for the reactions $e^+e^- \to \eta\pi^+\pi^-$ and $e^+e^- \to \omega\pi^0 \to \pi^+\pi^-\pi^0\pi^0$.

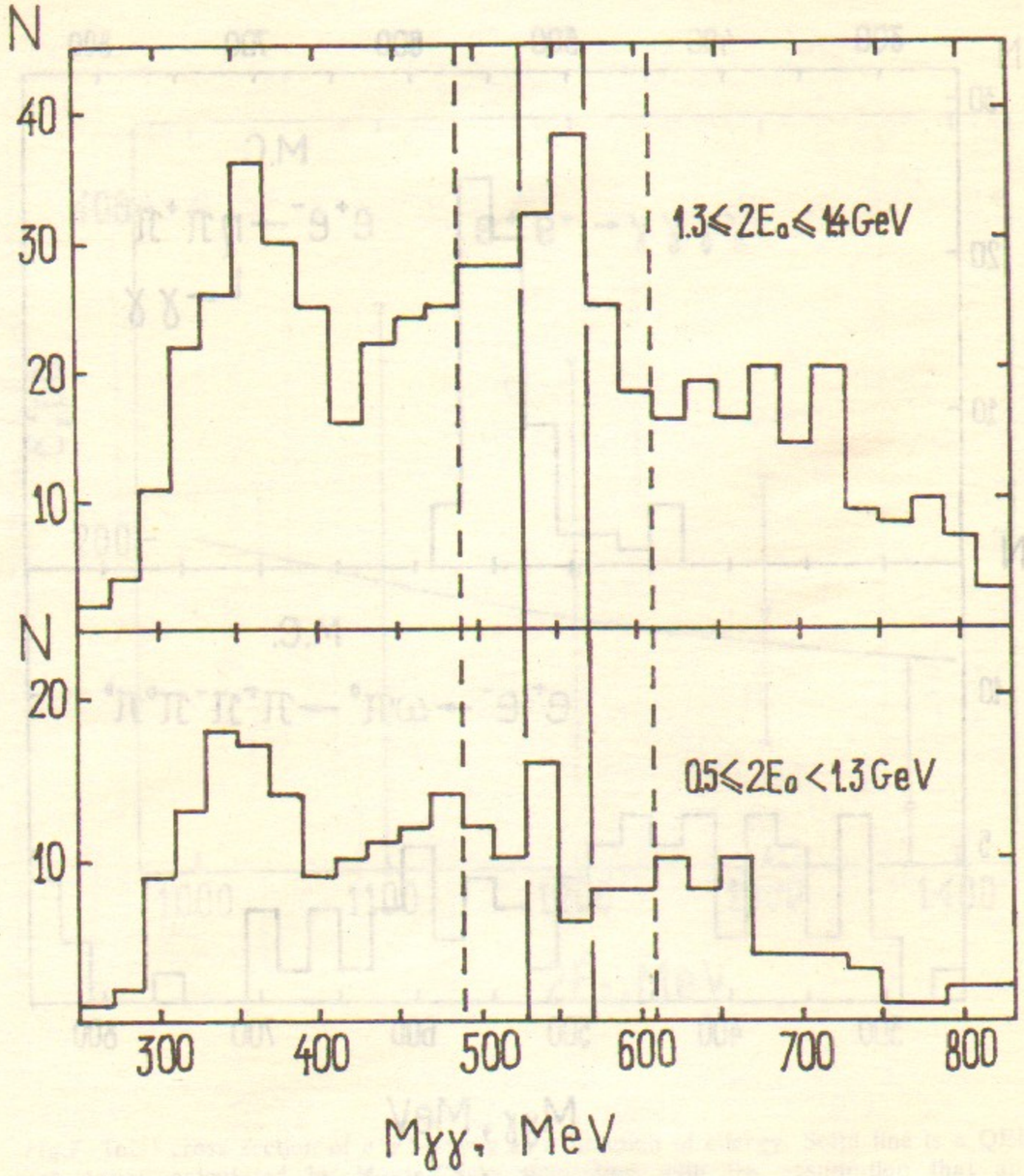

Fig.9. Measured two-photon invariant mass spectra in the energy intervals $1.05<2E_0<1.30$ GeV (*a*) and $1.30<2E_0<1.40$ GeV (*b*). The regions of «effect» and «background» for selection of $\eta\pi^+\pi^-$ events are shown by dotted lines.

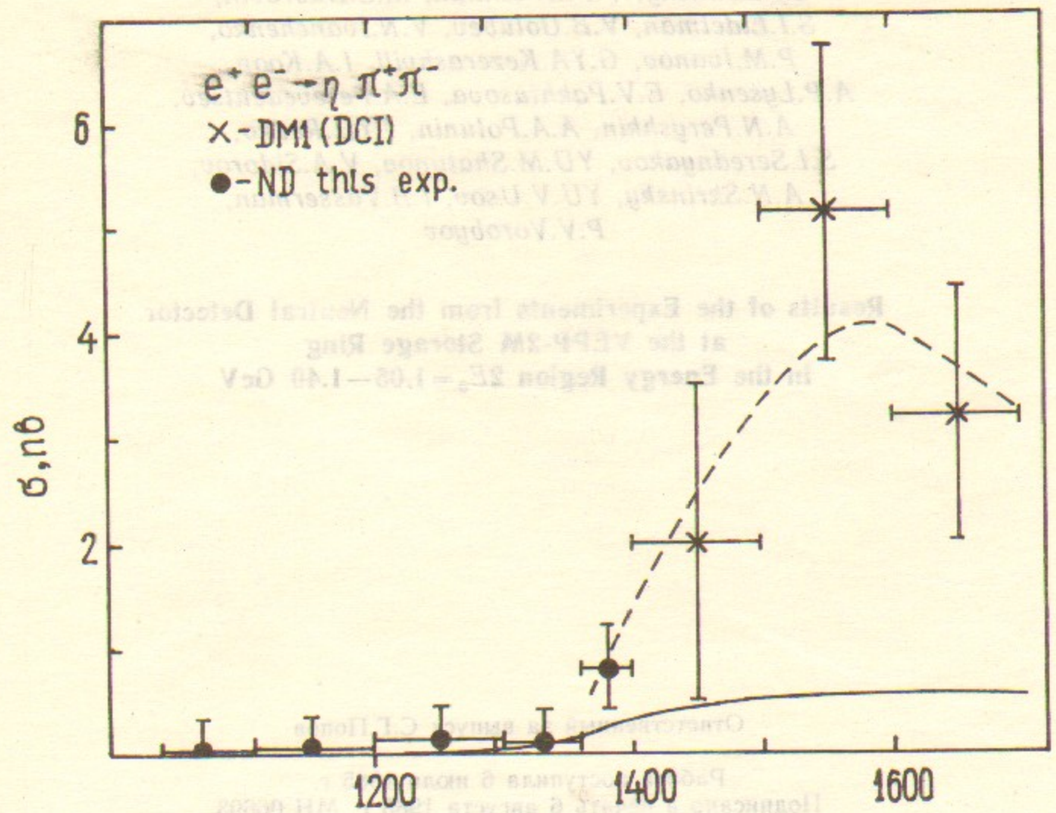

Fig.10. The total cross section of $e^+e^-\to\eta\pi^+\pi^-$ as a function of energy.

●—this paper, ×—DM1 results [29], solid line is a VDM prediction with only ϱ(770) taken into account [27], dotted line is an optimal excitation curve of ϱ′(1600) obtained in Ref. [29].

S.I.Dolinsky, V.P.Druzhinin, M.S.Dubrovin,
S.I.Eidelman, V.B.Golubev, V.N.Ivanchenko,
P.M.Ivanov, G.YA.Kezerashvili, I.A.Koop,
A.P.Lysenko, E.V.Pakhtusova, E.A.Perevedentsev,
A.N.Peryshkin, A.A.Polunin, I.YU.Redko,
S.I.Serednyakov, YU.M.Shatunov, V.A.Sidorov,
A.N.Skrinsky, YU.V.Usov, I.B.Vasserman,
P.V.Vorobyov

Results of the Experiments from the Neutral Detector at the VEPP-2M Storage Ring in the Energy Region $2E_0 = 1.05 - 1.40$ GeV

Ответственный за выпуск С.Г.Попов

Работа поступила 6 июля 1985 г.
Подписано в печать 6 августа 1985 г. МН 06693
Формат бумаги 60×90 1/16 Объем 2,2 печ.л., 1,8 уч.-изд.л.
Тираж 290 экз. Бесплатно. Заказ № 98

Набрано в автоматизированной системе на базе фотонаборного автомата ФА1000 и ЭВМ «Электроника» и отпечатано на ротапринте Института ядерной физики СО АН СССР,
Новосибирск, 630090, пр. академика Лаврентьева, 11.